Formation of Supported Membranes from Vesicles

C. A. Keller,[1] K. Glasmästar,[1] V. P. Zhdanov,[1,2] and B. Kasemo[1]

[1]*Department of Applied Physics, Chalmers University of Technology and Göteborg University, S-412 96 Göteborg, Sweden*
[2]*Boreskov Institute of Catalysis, Russian Academy of Sciences, Novosibirsk 630090, Russia*

(Received 14 October 1999)

Using a combination of the quartz crystal microbalance and surface plasmon resonance techniques, we have studied the spontaneous formation of supported lipid bilayers from small (~25 nm) unilamellar vesicles. Together these experimental methods measure the amount of lipid adsorbed on the surface and the amount of water trapped by the lipid. With this approach, we have, for the first time, been able to observe in detail the progression from the adsorption of intact vesicles to rupture and bilayer formation. Monte Carlo simulations reproduce the data.

PACS numbers: 87.16.Dg, 87.14.Cc, 87.15.Rn, 87.68.+z

An exciting prospect in the ongoing biotechnology revolution is the development of ways to accurately, quickly, and cheaply diagnose and treat disease by detecting vectors (proteins or DNA) that signal the presence of a disease or a drug. To accomplish this goal, we must understand the chemistry of healthy and diseased living systems and develop appropriate detection techniques. Supported membranes, a lipid bilayer supported on a solid substrate, are part of both of these efforts. They serve as model membranes in the study of cellular processes [1,2], and as biosensor components [3]. In biosensors, supported membranes provide high sensitivity by allowing immobilization of active proteins (receptors) at an adsorption resistant interface. While much effort has been put into the production and characterization of different types of supported membranes, comparatively little has been aimed at understanding the processes by which they form [4–6]. Here we present a detailed experimental study of the formation of supported membranes on SiO_2 from small unilamellar vesicles. This is currently the most common and most robust way of forming high quality supported lipid bilayers.

Small unilamellar vesicles (SUVs) (12.5 nm radius) are prepared by sonication of egg phosphatidylcholine suspended in buffer (100 m*M* NaCl, 10 m*M* Tris, pH 8.0) [2,7]. A clean SiO_2 surface evaporated onto a quartz crystal microbalance (QCM) crystal or a surface plasmon resonance (SPR) chip is mounted in a liquid cell and exposed to flowing buffer. Adsorption is initiated by replacing the buffer with buffer containing vesicles.

Figure 1 shows QCM and SPR data for the adsorption of lipid vesicles on a SiO_2 surface. The dramatic difference in the mass uptake (heavy lines) measured with QCM and SPR is due to the difference in sensitivity to trapped water. The QCM oscillates in a shear mode. Mass that becomes mechanically coupled to the surface of the QCM causes the resonant frequency (f) of this mode to decrease. The coupled mass includes adsorbed lipid, water trapped inside and between adsorbed vesicles, and a small amount of water adjacent to adsorbed vesicles. In contrast, the SPR technique measures the change in index of refraction near the surface as water is replaced by adsorbed lipid. Since the evanescent light wave sensing the adsorbed layer has an extinction depth an order of magnitude longer than the thickness of the lipid layer, SPR measures the mass of the adsorbed layer essentially independent of its morphology. Thus, the difference between the QCM and SPR curves corresponds to the total mass of water trapped at the surface by the lipid. We also measure the changes in energy dissipation (D) of the QCM (fine line in Fig. 1) due to changes in the viscoelastic and frictional properties of the adsorbing layer [10].

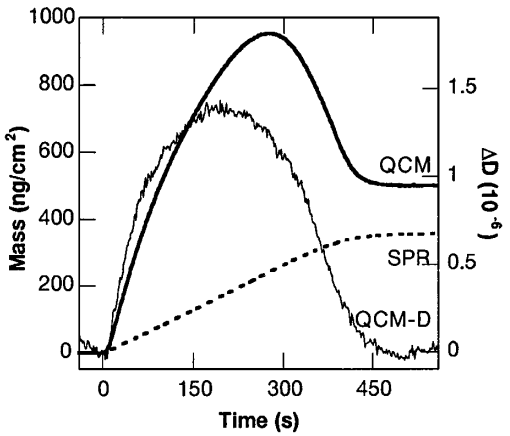

FIG. 1. QCM and SPR measurements of lipid bilayer formation on SiO_2 from 25 nm vesicles in solution. The left-hand scale shows the mass uptake (heavy lines) measured by SPR (lipid mass) and QCM (lipid mass + trapped water). The QCM energy dissipation signal (fine line, right-hand scale) is also shown. After bilayer completion, no change is observed in any of the signals upon rinsing with buffer. The extraordinary linearity of the adsorption of lipid as measured with SPR up to ~85% of the lipid required for a complete bilayer indicates that the adsorption rate is diffusion limited. To account for the different flow rates in the two experiments the time axis of the SPR data has been scaled to give the same total adsorption time as measured with the QCM. Both the QCM frequency and the SPR signals have been converted to mass/cm^2 (left-hand scale). For the QCM, 1 Hz = 18 ng/cm^2 [8]. For SPR, 1 RU = 0.092 ± 0.005 ng/cm^2 [9].

Following the adsorption process in Fig. 1 step by step, we see that when adsorption begins a large amount of water is trapped for each increment of lipid added to the surface. This corresponds to the adsorption of intact vesicles [11] at widely separated sites on the surface. As adsorption continues and the number of vesicles on the surface increases, the net water trapped per additional vesicle decreases until it reaches zero when the slope of the QCM measurement equals the slope of the SPR measurement (at $\sim$250 s in Fig. 1). Note that at this point the SPR data indicate that the rate of vesicle (lipid) adsorption is approximately the same as it was when adsorption began.

As adsorption continues, each added vesicle results in a net loss of trapped water. This mass loss overcompensates the addition of lipid mass giving the mass loss observed in the QCM measurements. Presumably, both the breaking of vesicles and the closer packing of intact vesicles on the surface contribute to the steady decrease in the water trapped per added vesicle. Packing is important because each vesicle is hydrodynamically coupled to the nearby water; as more vesicles adsorb on the surface, the volumes of water interacting with individual vesicles begin to overlap, thereby decreasing the average volume of water coupled to the surface per vesicle.

Theory indicates that there is a minimum radius for the rupture of a single vesicle sitting on a surface [5] and that vesicle decomposition is thermodynamically facilitated near the edge of an adsorbed lipid bilayer [12]. On mica, atomic force microscope (AFM) measurements [6] show that when small vesicles sit close together, they can fuse to form larger vesicles; when fusion produces a vesicle larger than the minimum radius for rupture, the vesicle breaks. We will show that without the addition of more vesicles from solution small vesicles on the surface are stable—a result that is completely consistent with the AFM observations and that places a lower bound on the minimum radius for rupture. (Note that this process is surface specific; e.g., on oxidized gold, vesicles do not fuse but stay intact even at saturation coverage [11].)

The picture of the adsorption process outlined above is supported by the QCM dissipation measurements. Initially, as intact vesicles accumulate on the surface, the dissipation increases due to deformation of the nonrigid, water rich overlayer by the shear oscillation. The deformation gives rise to both internal and interfacial frictional losses. As (after the f maximum) the relatively rigid lipid bilayer forms from the adsorbed vesicles, the dissipation decreases.

After completion of the supported lipid bilayer, the difference between the adsorbed mass measured with the QCM and SPR indicates that there is still a significant amount of water associated with the bilayer. This includes water molecules within the bilayer, water associated with the lipid head groups, water trapped between the surface of the sample and the proximal surface of the bilayer, and water trapped in the small number of intact vesicles that may remain stuck to the surface.

There are two simple explanations for the peak in the QCM data. (i) If the lifetime of a vesicle on the surface is long relative to the adsorption time scale, then vesicles will accumulate on the surface before vesicles begin to break, a peak in the adsorbed mass will be observed, and the peak height will vary with the adsorption rate. (ii) If vesicles on the surface break when a critical density of vesicles has accumulated on the surface, then a peak will occur if the accumulated mass (lipid plus water) at the critical density is greater than the mass of a completed bilayer, and the peak height will be independent of the adsorption rate. Figure 2 shows the adsorption kinetics measured by QCM and SPR for vesicle concentrations that vary by over 3 orders of magnitude. The large range of corresponding adsorption rates allows us to determine the source of the peak in the QCM data. As the data in Fig. 2a show, the peak height does not vary with adsorption rate. Thus, vesicle breakage begins at a critical density of vesicles on the surface.

Figure 2 also shows that the entire adsorption process scales with exposure of the surface to vesicles (vesicle concentration $\times$ time). Thus, the entire adsorption process is essentially time independent. The formation of a lipid bilayer occurs in two parts, (i) vesicle adsorption and

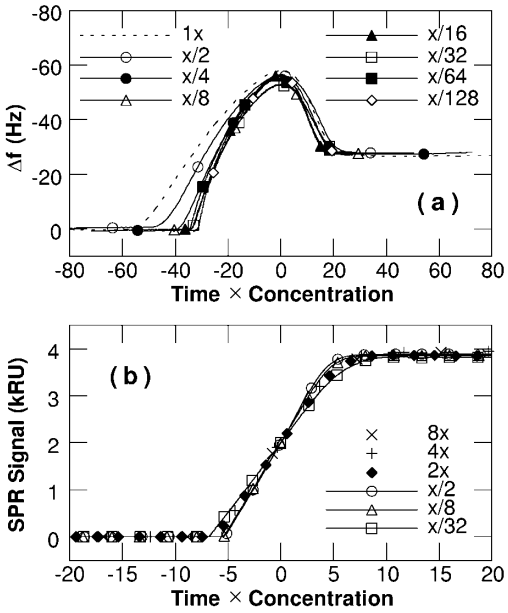

FIG. 2. Adsorption vs exposure for different concentrations of vesicles in solution. (a) QCM and (b) SPR data are shown for adsorption from vesicle solutions with concentrations from $x/128$ to $8x$; x is our reference concentration of 126 ng/μl (164 μM) of lipid in buffer. The corresponding times for completion of the bilayer range from 110 min to 3 s and the adsorption rates cover a 2200-fold range. This plot demonstrates that all parts of the adsorption process scale with exposure (vesicle concentration $\times$ time) to vesicles in solution. The small spread before the peak in the QCM data at high concentrations is due to the time required for complete exchange of the solution in the measurement cell.

(ii) rupture and fusion. Surprisingly, both of these processes scale with exposure to vesicles in solution implying that vesicle fusion and rupture are both driven by the adsorption of vesicles from solution.

In Fig. 3, the QCM data of Fig. 2a are plotted in a time independent manner by utilizing the dissipation measurement. This shows that the path traced out through the f-D plane during the adsorption process is independent of the concentration of vesicles in solution and independent of how fast the progression from low to high coverage occurs. This has interesting consequences. Generally, if the same amount of material is adsorbed on two surfaces but in different forms, each will give approximately the same frequency shift but a different dissipation shift. Thus, a given point in the f-D plane corresponds to a given state of the surface and Fig. 3 allows us to deduce that the system always passes through the same set of states during the adsorption process even when the rate of formation is varied a hundredfold.

To provide a more complete picture, we have also performed experiments where the adsorption process is interrupted before completion of the bilayer by switching from buffer plus vesicles to pure buffer. After any transients associated with the interruption, we switch back to buffer plus vesicles whereupon the formation of a bilayer continues to completion.

The SPR experiments (Fig. 4a) show that upon interruption, adsorption of lipid simply stops. This is independent of where interruption occurs in the adsorption process. Most importantly, after interruption, at any coverage, lipid does not desorb. Thus, since SPR is not sensitive to morphological changes in the adsorbed layer that conserve the adsorbed lipid mass, the adsorption of lipid on SiO_2 is irreversible and the "mass loss" observed with the QCM (Fig. 2a) is due entirely to loss of trapped water.

The results of similar interruption experiments with the QCM are shown in Fig. 4b. When interruption occurs at or before the peak, the result is similar to that of the SPR experiments; the adsorption process simply stops, and, after interruption, the system is stable. This confirms our previous conclusion that vesicles do not spontaneously break on the SiO_2 surface but begin to break after a threshold density of vesicles is reached on the surface. When interruption occurs after the peak, the mass coupled to the QCM continues to decrease after the interruption but stops before reaching that of a complete bilayer. This indicates that something causes the breaking of vesicles to continue for a short time after the vesicles have been removed from solution. While our simulations [13] show that this behavior can be explained by vesicle decomposition due to interaction with nearby islands of lipid bilayer, we cannot eliminate other mechanisms. In particular, recent AFM experiments [6] on mica indicate that the vesicles used in our experiments are too small to rupture without first reaching a critical density where they fuse to form larger vesicles that then break to form the bilayer. If the time required for fusion is sufficiently long, this process may contribute to the vesicle breakage observed after the adsorption is interrupted. This would imply that the time to fusion increases rapidly with the distance between vesicles.

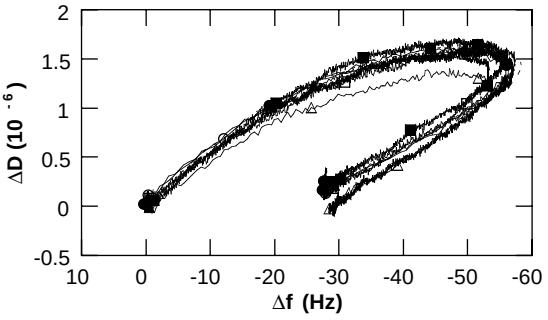

FIG. 3. Plots of D vs f for the QCM data of Fig. 2a. The plot shows that time can be eliminated as an important parameter; i.e., the governing parameter is exposure, not time.

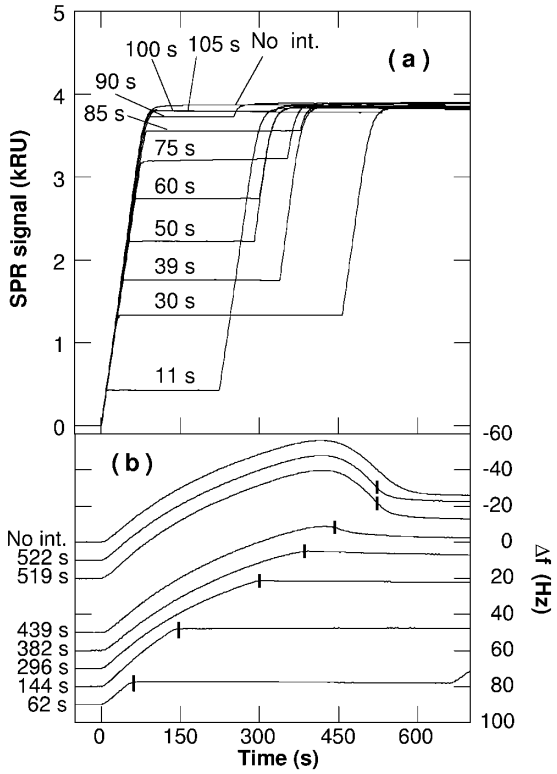

FIG. 4. (a) SPR and (b) QCM data for interruption experiments. Vesicles are introduced at time zero. The curves are labeled with the interruption time. The small vertical bars in (b) indicate the points where the adsorption was interrupted by removal of vesicles from solution. Note in (b) that before the maximum, the QCM signal stays constant after an interruption, but when the interruption occurs after the maximum, it decreases after the interruption. In all cases, completion of the bilayer occurs upon a second addition of vesicles. This is shown for the SPR data but not for the QCM data except for the QCM run interrupted at 62 s where the upturn after 600 s is due to the second addition.

Since, after interruption, the measured change in frequency is still greater than that of a complete bilayer, we know that there are still intact vesicles on the surface. At the same time, the SPR data indicate that there is not enough lipid on the surface to form a complete bilayer. Thus, the transition from vesicles to bilayer requires continued adsorption of vesicles from solution, both to drive the breaking of vesicles and to supply the lipid needed to complete the bilayer.

We have performed Monte Carlo simulations of the vesicle adsorption and fusion processes that support our picture of the overall adsorption and fusion process. The model includes diffusion-limited adsorption of vesicles and spontaneous, adsorption-induced, and membrane-induced decomposition of adsorbed vesicles. It reproduces the QCM and the SPR experiments presented here, including the interruption experiments. The model is described in detail in Ref. [13].

Methods.—The concentration of lipid in each SUV preparation was obtained by measuring the phosphate content after converting it to an inorganic form [14]. The concentrations ranged from 10 to 20 mg/ml. The hydrodynamic radius of the vesicles was measured by photon correlation spectroscopy and agrees with previous work [7,15]. The internal surfaces of both measurement systems were precoated with lipid before each set of experiments. All experiments were performed at $21.8 \pm 0.1\,^{\circ}\mathrm{C}$. The flow rate through the measurement cell was 6.67 ml/min for the QCM experiments and 40 μl/min for the SPR experiments.

We used 2.54 cm diameter, 5 MHz, QCM crystals. The resonant frequency and dissipation were measured at $\sim$1 s intervals [10]. In this paper, we have assumed that the change in resonant frequency is proportional to the adsorbed mass (the Sauerbrey equation) [16]. Although this is not strictly true for the adsorption of dissipative structures such as vesicles, for the work presented here the deviations are not expected to be larger than a few percent [17] and do not affect our conclusions.

A detailed account of the SPR techniques used in the BIAcore2000 system can be found in Ref. [18].

We thank Per Borchardt for lab work, Kristin Mjörn for an introduction to the utility of SPR, Hans Elwing for access to his SPR system, and Fredrik Höök and Duncan Sutherland for many valuable suggestions and discussions. This work was supported by the Biomaterials Consortium (SSF and NUTEK) and TFR.

[1] J. D. Burgess *et al.,* Langmuir **14**, 2467 (1998); S. Heyse *et al.,* Biochemistry **37**, 507 (1998).
[2] J. Salafsky *et al.,* Biochemistry **35**, 14 773 (1996).
[3] E. Sackmann, Science **271**, 43 (1996).
[4] G. Brink *et al.,* Biochim. Biophys. Acta **1196**, 227 (1994); E. Kalb *et al., ibid.* **1103**, 307 (1992); C. Steinem *et al., ibid.* **1279**, 169 (1996); T. J. Feder *et al.,* Phys. Rev. E **51**, 3427 (1995); S. Heyse *et al.,* Protein Sci. **4**, 2532 (1995); H. Lang *et al.,* Thin Solid Films **210/211**, 818 (1992); Langmuir **10**, 197 (1994); J. B. Hubbard *et al.,* Biophys. Chem. **75**, 163 (1998); P. S. Cremer and S. G. Boxer, J. Phys. Chem. B **103**, 2554 (1999).
[5] U. Seifert and R. Lipowsky, Phys. Rev. A **42**, 4768 (1990); U. Seifert, Adv. Phys. **46**, 13 (1997).
[6] I. Reviakine and A. Brisson, Langmuir **16**, 1806 (2000).
[7] Y. Barenholz *et al.,* Biochemistry **16**, 2806 (1977).
[8] C. Lu and A. W. Czanderna, *Applications of Piezoelectric Quartz Crystal Microbalances* (Elsevier Science, Amsterdam, 1984).
[9] M. A. Cooper *et al.,* Biochim. Biophys. Acta **1373**, 101 (1998).
[10] M. Rodahl *et al.,* Rev. Sci. Instrum. **66**, 3924 (1995).
[11] C. A. Keller and B. Kasemo, Biophys. J. **75**, 1397 (1998).
[12] V. P. Zhdanov (unpublished).
[13] V. P. Zhdanov *et al.,* J. Chem. Phys. **112**, 900 (2000).
[14] *Manual on Membrane Lipids, Springer Lab Manual,* edited by R. Prasad (Springer, Berlin, 1996).
[15] C.-H. Huang, Biochemistry **8**, 344 (1969).
[16] G. Sauerbrey, Z. Phys. **155**, 206 (1959).
[17] M. Rodahl *et al.,* Faraday Discussions **107**, 229 (1997).
[18] E. Stenberg *et al.,* J. Colloid Interface Sci. **143**, 513 (1991); I. Lundström, Biosen. Bioelectron. **9**, 725 (1994).